Proceedings of the Sixth International Conference on
Railway Technology: Research, Development and Maintenance
Edited by: J. Pombo
Civil-Comp Conferences, Volume 7, Paper 5.5
Civil-Comp Press, Edinburgh, United Kingdom, 2024
ISSN: 2753-3239, doi: 10.4203/ccc.7.5.5

Optimization of Primary Suspension of Freight Wagons to Improve Wheel Wear and Rolling Contact Fatigue

C. Suque Endlich[1], M. Valente Lopes[1], P. Augusto De Paula Pacheco[1,2] and A. Antunes Dos Santos[1]

[1]School of Mechanical Engineering
State University of Campinas, Brazil
[2]Railway Department, Federal Institute of Education Science and Technology of the Southeast of Minas Gerais
Brazil

Abstract

From freight rail speed and load increasing, wheel wear becomes increasingly significant. One of the approaches to reduce wheel wear is using a rubber pad adapter between the wheelset bearing and the side frame pedestal, as a part of the primary suspension. In this paper, a method is proposed to optimize the pad proprieties: stiffness and clearance. A heavy-haul wagon multibody vehicle dynamic model is established in SIMPACK, and the non-dominated sorting genetic algorithm-II (NSGA-II) is used to optimise the pad proprieties. The objective is to minimize the wear and the fatigue index while fulfilling objective restrictions. The analysis focuses on the sharp curve, 281.66 m radius, representative of a heavy haul Brazilian railway. The study resulted in two optimum pad designs, which prevented the wheel flange from contacting the rail during the curve. The solution can improve wear and fatigue indices up to 97.52% and 54.62%, based on the results. The optimal wear performance was achieved when longitudinal stiffness decreased by 68.14%, coupled with a 215.62% increase in longitudinal clearance. Additionally, lateral stiffness and clearance exhibited increases of 21.92% and 497.14%, respectively. Furthermore, there was a significant reduction in vertical (90%) and yaw (46.33%) stiffness.

Keywords: railway vehicle dynamics, wheel-rail interaction, multibody simulation, wear index, life extension, hunting stability.

1 Introduction

The wheelset is a high-cost component and usually requires high maintenance costs [1] due to its importance to safe and efficient transportation. In recent years, several studies have appeared to extend the wheel service cycle, thus enabling reduced maintenance costs [2]. These works detail the search for the best design for the whole system or specific parts of the wheelset, using optimisation techniques and reaching adequate results for improving safety and performance. Many optimization methods were used by the railway industry and academic community to improve suspension performance [3, 4], wheel and rail profiles [5-8], design [9, 10] and logistics [11, 12].

The wheelset, being a rigid body, moves laterally in the opposite direction to the curve, due to the conicity of the wheel. This movement brings the flange of the outer wheel of the curve closer to the inner face of the rail. Depending on factors such as speed, irregularities, gauge variation and curve radius, the flange may come into contact with the rail, intensifying the wear on the flange [13]. The wheel flange's wear limit needs to be controlled to ensure sufficient thickness to support lateral force and prevent derailment [14]. Furthermore, according to Zhang et al. [15], controlling the flange wear is important to reduce the removal material during the reprofiling, since for every 1 mm of wear on the flange, it is necessary to remove up to 4.2 mm in wheel diameter.

To improve wheel-rail contact (W/R) in curves and, consequently, reduce flange wear, an element was added to the primary suspension. Known as a “shear pad”, it is placed between the wheelset bearing and the side frame pedestal (Figure 1). This pad allows movement between the wheelset and the side frame, facilitating the alignment of the wheelset when negotiating the curve [16].

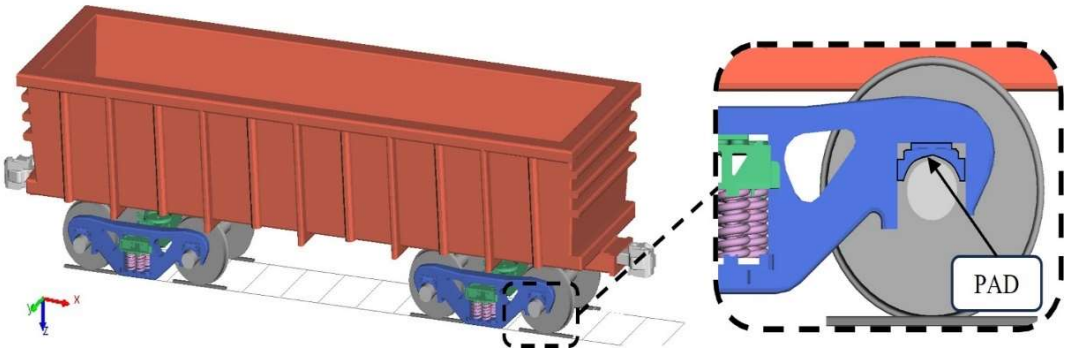

Figure 1: GDE-Ride Control with pad model designed with SIMPACK®.

Lima et al. [17] analyzed the dynamic behaviour of a bogie with and without a pad. It was observed that the pad reduces the wheelset's angle of attack and causes a considerable decrease in the amplitude of the lateral oscillations after the transition curve. Furthermore, they concluded that longitudinal stiffness is what most impacts the dynamics during the curve. Under these results, Correa et al. [16] found that the longitudinal stiffness of the primary suspension of heavy-haul vehicles is the one which has the greatest impact on safety and wear parameters. They use sensitivity analysis and multibody dynamic simulation to evaluate a heavy haul vehicle, like the

one under study in the present work. Pacheco et al. [18] used multiple linear regression to examine the relationship between longitudinal and lateral stiffness and clearance of the pad and wear volume. It was found that the parameters related to the longitudinal dynamics counted significantly in determining the wear volume, i.e. reducing stiffness, and increasing the gap reduces wear.

In this work, the methodology proposed by Pacheco et al. [5] is applied to a Brazilian metric-gauge heavy-haul railroad to obtain optimized pad properties. The methodology created employs NSGA-II (Non-dominated Sorting Genetic Algorithm II) in combination with multibody dynamic simulation to find the best pad parameters aiming to reduce wear and fatigue.

In the subsequent sections of this article, Section II outlines the applied method, encompassing specificities of multibody simulation, NSGA-II algorithm, and the procedure for data analysis. Section III is dedicated to discussing the results, and Section IV provides the conclusions.

2 Methods

In this section, the optimization method is presented, aligned with the previously outlined objectives. The focus is on enhancing the efficiency of wheel-rail interactions. The section is organized as follows: the dynamic model of the wagon using the software SIMPACK® is given in Sec. (2.1); Sec. (2.2) presents the NSGA-II algorithm; and finally, in Sec. (2.3), the optimization method is outlined.

2.1 Dynamic Model

A wagon with a three-piece bogie (GDE-Ride Control) with 27.5 tons per axle was modelled in SIMPACK®, for dynamic evaluation. The model has already been applied and validated in previous works [16, 18, 19].

The wheel/rail (W/R) contact method employed is the equivalent elastic. This method was chosen to reduce simulation time, due to the large number of simulations required. It uses an elliptical approximation of the contact area and calculates a penetration equivalent to that area. From this penetration, the normal and tangential forces are calculated by Hertz and FASTSIM, respectively. According to Vollebregt [20], this method is sufficiently accurate for predicting hunting, derailment, tensile forces, excitations, and fatigue of components.

In Figure 2, the three force elements with stiffness and damping used to model the pad are presented. The element located in the centre of the pad is bushing type. This element applies stiffness and damping forces in the x and y directions, as well as torque in the rotation in z. The other two force elements are translational only, being applied only in the z-direction. For stiffness, a force is applied as a function of clearance and its variation is shown in Figure 3.

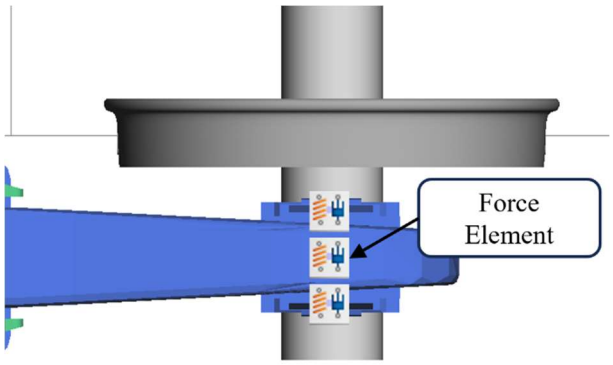

Figure 2: Pad model as force elements in SIMPACK®.

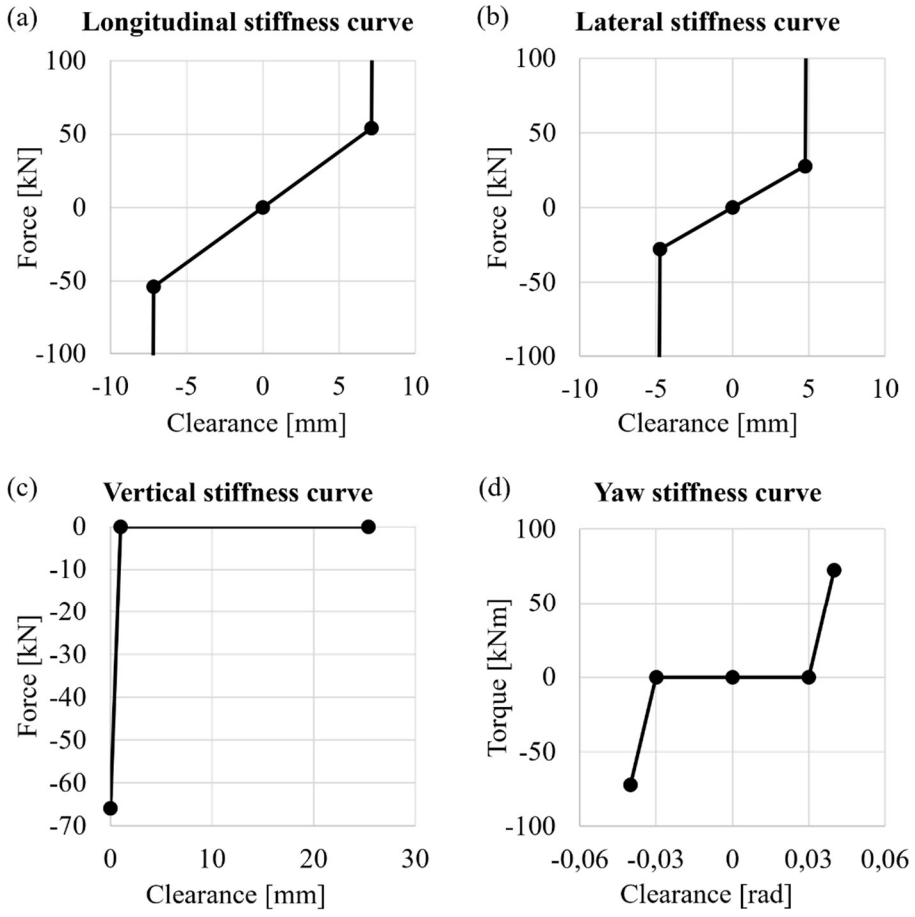

Figure 3: Stiffness characteristic curves for the GDE-Ride Control wagon. (a) Longitudinal; (b) Lateral; (c) Vertical; (d) Yaw torque.

For the dynamic analysis, the sharpest curve of the railway under study was selected. The reference track is composed of a straight section (150 m), an entry curve transition (81.40 m) defined as a linear clothoid, a full curve to the left of 281.66 m radius (140.20 m in length), an exit curve transition (81.40 m), then a straight section (230

m) to end (see Figure 4). The selected rail profile is TR68, and the wheel profile is AAR 1:20.

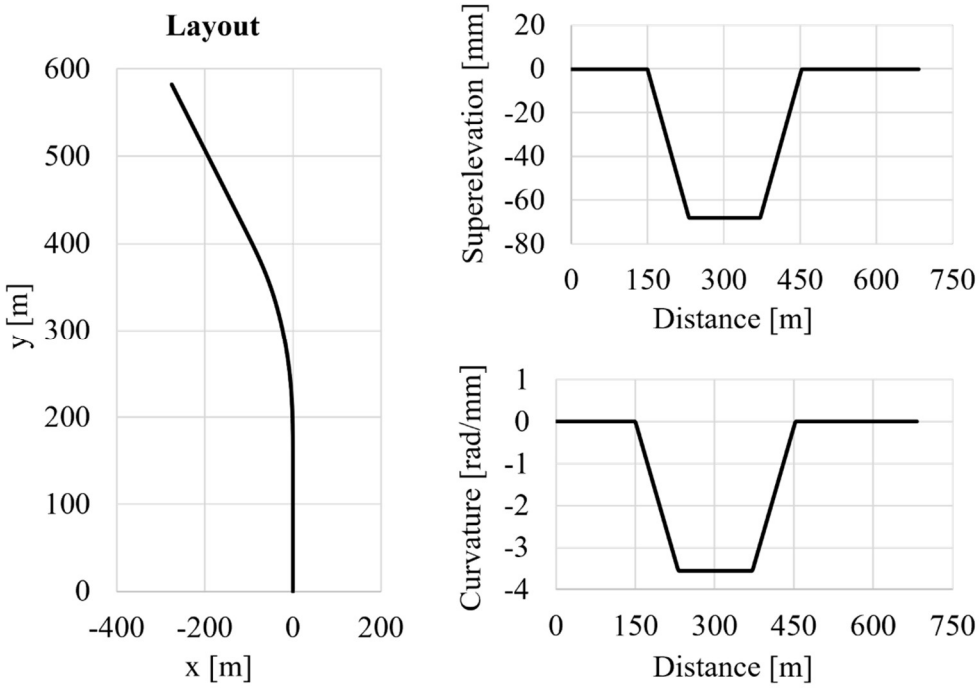

Figure 4: Designed track layout, curvature, and superelevation.

2.2 NSGA-II

Deb et al. [21] improved the NSGA (Non-Dominant Selection Genetic Algorithm) optimization method to reduce computational time, generating the NSGA-II, which makes it possible to be employed with larger populations. Based on an elitist dominance ranking (Pareto ranking), it preserves the best individuals from the current and previous populations. Crowding distance ensures the diversity of optimal candidates [7].

From an initial random population of size N, a population of descendants of the same size is created through processes of crossover and mutation. The union of these populations forms a generation of size $2N$. These individuals are then classified according to the Pareto frontier and the crowding distance. Afterwards, half of the generation is eliminated. The process of creating a new generation is then repeated, resulting in the classification of the best individuals from the previous one.

The NSGAII algorithm was implemented using the MATLAB® platform, and simulations were conducted using SIMPACK® software. The population size is 288 and the number of generations is 200. Distribution indices for cross-over and mutation are chosen as $\eta_{cross\_over} = 0.1$ and $\eta_{mutation} = 0.1$, respectively.

2.3 Optimization method

The optimization variables are longitudinal stiffness (k_x), lateral stiffness (k_y), absolute maximum vertical force (F_z), absolute maximum yaw torque (T_{yaw}), and clearance in x (f_x) and y (f_y) directions. For damping, adjustments were made, making it proportional to the variations in the stiffness curve over the benchmark. Consequently, the damping is also adjusted. This modification ensures that all properties in that specific direction are changed by the same factor, guaranteeing model consistency.

The pad optimization problem is defined based on [6].

Minimize:

$$\text{Wear index: } f1 = \frac{1}{675}\int_0^{675}\left(F_x v_x + F_y v_y\right)dS \text{ [N]}, \quad (1)$$

and

$$\text{Fatigue index: } f2 = \frac{1}{675}\int_0^{675}\left(\mu - {}^{k}/_{P_0}\right)dS \text{ [dimensionless]}. \quad (2)$$

$F_x \cdot v_x$ represents the product of the longitudinal creep force and the longitudinal creepage, and $F_y \cdot v_y$ refers to the lateral component. For the fatigue index, k is the shear yield limit, P_0 is the maximum Hertzian contact pressure and μ is the adhesion coefficient. The wear number and fatigue index are selected as the integral average along the length of the curve. The values of interest were collected on the right wheel of the first wheelset, which features the highest wear.

Subject to:

$g1$ = Lateral force: $Y \leq 132.625$ [kN].

$g2$ = Vertical force: $Q \leq 273.9375$ [kN].

$g3$ = Nadal criterion: $Y/Q \leq 0.8$ [dimensionless].

$g4$ = Contact pressure: $P \leq 2.5$ [GPa].

$g5$ = Maximum lateral acceleration: $\ddot{y}_{max} \leq 3.5$ [m/s²].

$g6$ = RMS of lateral acceleration: $\ddot{y}_{rms} \leq 1.3$ [m/s²].

$g7$ = Maximum vertical acceleration: $\ddot{z}_{max} \leq 5$ [m/s²].

$g8$ = RMS of lateral acceleration: $\ddot{z}_{rms} \leq 2$ [m/s²].

$g9$ = Acceleration stability: $sd_{lateral} = 0.01\ \left[\frac{\text{m}}{\text{s}^2}\right]$ and $sd_{vertical} = 0.05\ \left[\frac{\text{m}}{\text{s}^2}\right]$.

The constraints *g1–g4* were based on [6], but the maximum value in the curve section (150 – 453 m) and the tangent section (455 – 675 m) were used.

The other constraints were established by focusing on managing the lateral and vertical acceleration, as this is crucial for ensuring a safe ride. The acceleration in

railway dynamics is influenced by track design elements such as curve radius, cant, and superelevation, along with the wagon's speed, irregularity, wheel and rail profiles, and the suspension system. However, in this work, just the primary suspension was altered, and track irregularities were not considered.

The *g5–g8* restrictions were defined according to UIC 518 [22], where the absolute maximum acceleration and the root means square value (rms) in the curve section (150 – 453 m) and the tangent section (455 – 675 m) were used.

Wu et al. [23] established a criterion for hunting instability that compares the lateral acceleration under normal and hunting conditions in different vehicle models. This criterion considers the peak acceleration and the number of times the signal continuously exceeds a threshold, which is observed to occur 6 times within a 15 s interval. Therefore, the g9 restriction stipulates that the acceleration peak signal can exceed sd m/s² above its average no more than six times consecutively. In this work, peak acceleration values were obtained in the curve section (250 – 365 m) and the tangent section (455 – 675 m), provided the duration is under 15 s. The threshold is set with the assumption that lateral and vertical accelerations will remain stable under conditions of constant curvature as the result found for the pad currently used in the railway.

3 Results

Following the implementation of the methodology, the resultant dispersion graph of the generated population and the Pareto frontier were created. Figure 5 correlates the two objective functions, $f1$ (average integral of wear index) and $f2$ (average integral of RCF index). It selectively displays only those solutions that conform to the established constraints of this study.

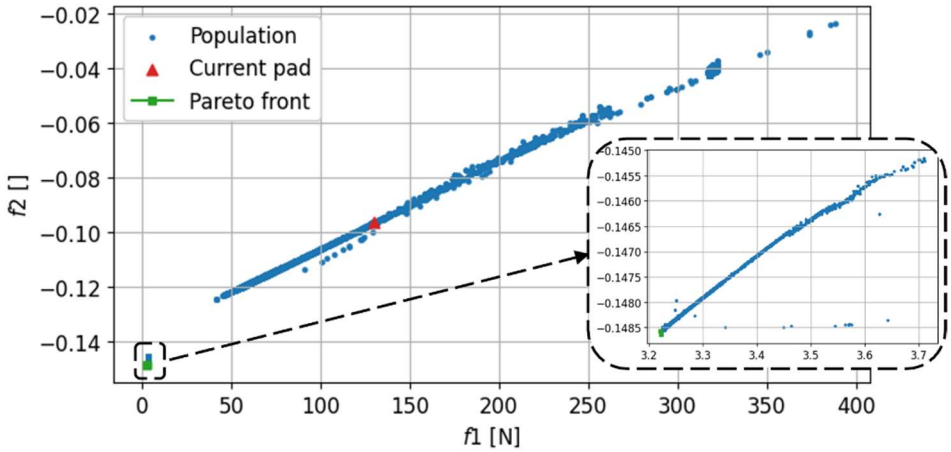

Figure 5: Dispersion graph of the population with the current pad.

It has been observed that a significant portion of the population, approximately 15.75%, tends to cluster within a specific range, with $f1$ values between -0.14516 and -0.14864, and $f2$ values ranging from 3.2217 to 3.7109 N. This stratified sample, referred to as Sample 1, represents the part of the population that has just one contact point on the curve, indicating no contact on the flange during the curve.

Figure 6 illustrates the distribution of suspension-related variables for Sample 1. Variables associated with clearance display a broader interquartile range. Additionally, k_x, k_y, F_z and T_{yaw} exhibit a more constrained distribution. This indicates that the clearance parameters have a wider range of acceptable values, showcasing greater variability and flexibility in attaining outcomes that are closely aligned with the Pareto front.

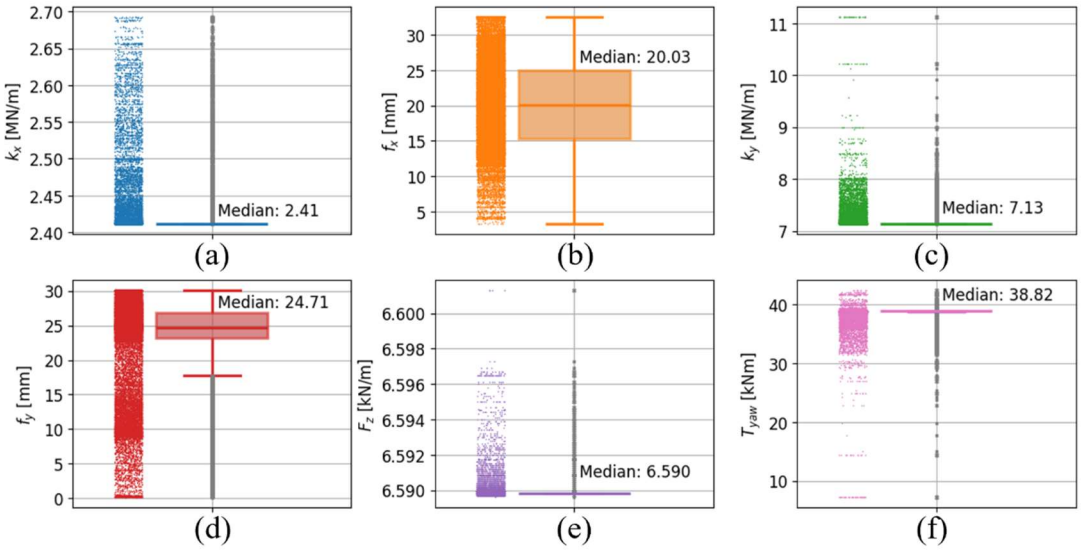

Figure 6: Distribution of pad parameters for the stratified sample with one point of contact (Sample 1)

Figure 7 presents an enlarged perspective, enhancing the visualization of the Pareto frontier. Within this frontier, only two individuals are featured. These individuals have been subjected to simulation and comparative analysis with the current pad. Onwards they are referred to as "Minimum T_γ" and "Minimum FI".

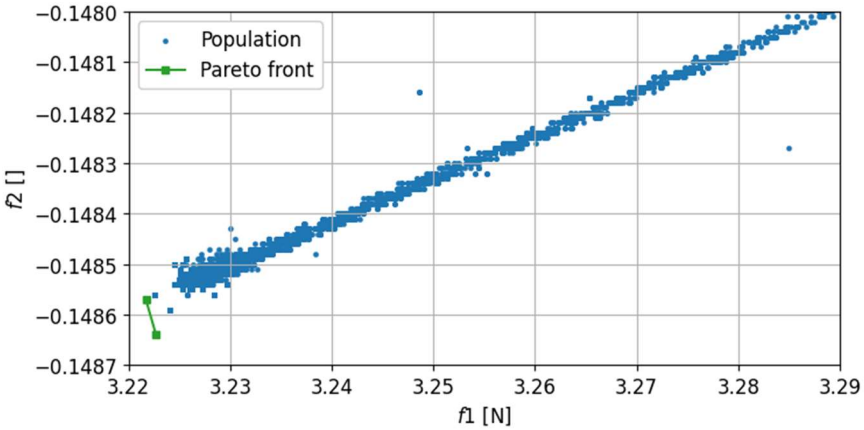

Figure 7: Detailed view of the Pareto Frontier.

Table 1 presents the $f1$ and $f2$ values obtained from this analysis. It was observed that considering the constraints of the problem, $f1$ decreased by 97.52%, while $f2$ experienced an average reduction of 54.62%. In other words, there was a decrease in wear and in the tendency towards fatigue.

	$f1$ [N]	**$f2$ [dimensionless]**
Current pad	129.7512	-0.09611
Minimum T_γ	3.2217	-0.14857
Minimum FI	3.2227	-0.14864

Table 1: Values of the objective functions obtained during the optimization process.

Table 2 shows that the longitudinal stiffness decreased by 68.14%, while the clearance experienced an increase of 215.62% for Minimum T_γ and 114.17% for Minimum FI. The lateral stiffness exhibited an increase of approximately 21.93%. In parallel, the clearance in the lateral direction increased by 497.14% for Minimum T_γ and 461.16% for Minimum FI. For the maximum absolute vertical force (F_z) and yaw torque (T_{yaw}), there was a significant reduction of 90% and 46.33%, respectively. Note that the Pareto design parameters are close to the medians of sample 1 shown in Figure 6.

	k_x [kN/m]	**f_x [mm]**	**k_y [kN/m]**	**f_y [mm]**	**F_z [kN]**	**T_{yaw} [kNm]**
Current pad	7569.33	7.140	5852.73	4.760	65.898	72.310
Minimum T_γ	2411.90	22.535	7136.30	28.424	6.5898	38.807
Minimum *FI*	2411.80	17.148	7135.70	26.711	6.5898	38.811

Table 2: Optimized property values on the Pareto frontier compared to the current pad.

The behaviour of T_γ and FI relative to distance travelled, as shown in Figures 8 and 9, validate the optimization of primary suspension parameters and the enhancement of the objective function, reaching the objectives of this work. Furthermore, it is observed that individuals on the Pareto frontier achieved nearly equivalent results.

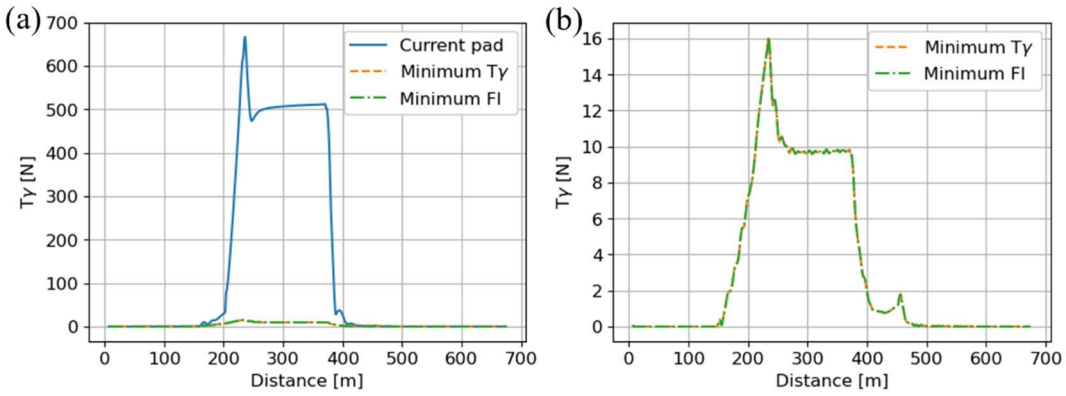

Figure 8: Comparison of the T_γ curve. a) Pareto design parameters compared with the current pad. b) Detail showing the behaviour of the best individuals.

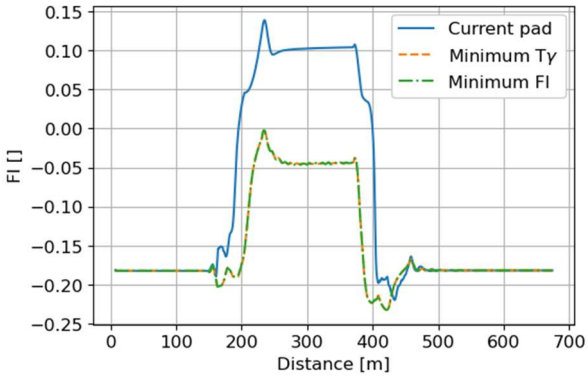

Figure 9: Comparison of the FI curve of the Pareto design parameters with the current pad.

Evaluating the lateral and vertical acceleration, presented in Figures 10 and 11, it is observed that the design for Minimum T_γ reduced the oscillation along the curve.

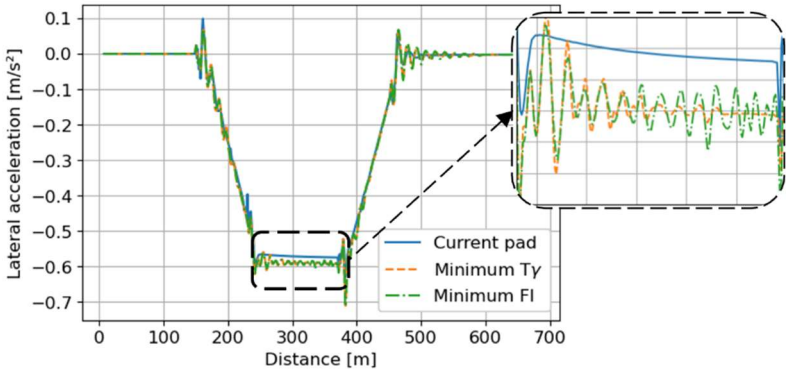

Figure 10: Comparison of the lateral acceleration curve of Pareto design parameters with the current pad.

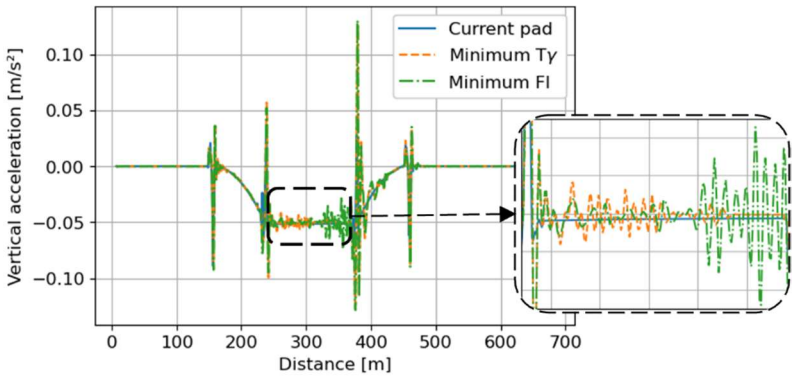

Figure 11: Comparison of the vertical acceleration curve of Pareto design parameters with the current pad.

Moreover, there was not a significant difference in the vertical acceleration between the current pad and the optimized individuals. However, it is noteworthy that the average lateral acceleration during the curve decreased by approximately 0.0177 m/s², remaining within the requirements of the standard.

5 Conclusion

This study employed optimization techniques and dynamic simulation to find the best design parameters to reduce wear and fatigue in the contact between wheels and rails for GDE wagons. The optimization process effectively identified primary suspension parameters that significantly reduce wear by avoiding flange contact during a curve, for a particular track geometry. Among these results, the optimized designs presented a notable reduction in longitudinal stiffness (68.14%), vertical stiffness force (90%), and yaw stiffness torque (46.33%). Additionally, there was an increase in lateral stiffness (21.93%). Moreover, lateral and longitudinal clearance demonstrated a broader distribution compared to other variables.

Performing the analysis presented in this study required some adjustments in the models. As an example, implementing a stability criterion for acceleration, which limits acceleration signal peaks to not exceed the mean plus a specific standard deviation within a specific track section, proved to be an effective way to maintain the dynamic stability of the wagon. This approach ensured that the results obtained were consistent with the track conditions.

The Minimum T_γ stands out as the best-performing individual, primarily due to its more stable behaviour compared with the current and the other individuals on the Pareto frontier, it exhibits significant differences in terms of clearance. Specifically, the longitudinal clearance of Minimum T_γ increased by 215.62% compared to the current and by 23.91% compared to Minimum FI. In terms of lateral clearance, there was an increase of 497.14% relative to the current and 6.03% compared to the Minimum FI. These results underscore the effectiveness of Minimum T_γ in maintaining stability, despite considerable increases in clearance measurements. Furthermore, there was an improvement of 97.52% concerning wear, and the Fatigue Index improved by 54.58%.

It is important to note that the parameters found during the optimization are not based on real pads; they are proposals. So, the stiffness for the optimum design will require the development of new materials and new geometries, which can bring new challenges for the railway industry.

6 Future research

Future research shall focus on considering irregularities and worn-out measurement profiles of the wheel and rail, this will provide a more realistic result. Furthermore, the analysis of different curve radii is crucial for the applicability of optimized pad design.

Acknowledgements

The authors wish to express their acknowledgement to Vale S.A. for funding this study and technical support. Also, to CNPq (grant number 315304/2018-9), which funded partially this project.

Reference

[1] X. Wang, J. Yuan, S. Hua e B. Duan, "Optimization of wheel reprofiling based on the improved NSGA-II," Hindawi, 2020.

[2] Y. Lu, Y. Yang, J. Wang, and B. Zhu, 'Optimization and Design of a Railway Wheel Profile Based on Interval Uncertainty to Reduce Circular Wear', Math Probl Eng, vol. 2020, p. 9579510, 2020, doi: 10.1155/2020/9579510.

[3] B. Allotta, L. Pugi, V. Colla, F. Bartolini, and F. Cangioli, "Design and optimization of a semi-active suspension system for railway applications," Journal of Modern Transportation, vol. 19, no. 4, pp. 223–232, Dec. 2011, doi: 10.3969/j.issn.2095-087X.2011.04.002.

[4] X. Chen, Y. Yao, L. Shen, and X. Zhang, "Multi-objective optimization of high-speed train suspension parameters for improving hunting stability," International Journal of Rail Transportation, vol. 10, no. 2, pp. 159–176, 2022, doi: 10.1080/23248378.2021.1904444.

[5] P. A. d. P. Pacheco, C. S. Endlich, K. L. S. Vieira, T. Reis, G. F. M. d. Santos e A. A. d. S. Júnior, "Optimization of heavy haul railway wheel profile based on rolling contact fatigue and wear performance," Wear,' vol. 522, 2023.

[6] A. C. Pires et al., "The effect of railway wheel wear on reprofiling and service life," Wear, vol. 477, Jul. 2021, doi: 10.1016/j.wear.2021.203799.

[7] I. Persson and S. Iwnicki, 'Optimisation of railway wheel profiles using a genetic algorithm', Vehicle System Dynamics, vol. 41, Jan. 2004.

[8] H. Y. Choi, D. H. Lee, and J. Lee, "Optimization of a railway wheel profile to minimize flange wear and surface fatigue," Wear, vol. 300, no. 1–2, pp. 225–233, Mar. 2013, doi: 10.1016/j.wear.2013.02.009.

[9] M. Mohebbi and M. A. Rezvani, "Multi objective optimization of aerodynamic design of high speed railway windbreaks using Lattice Boltzmann Method and wind tunnel test results," International Journal of Rail Transportation, vol. 6, no. 3, pp. 183–201, Jul. 2018, doi: 10.1080/23248378.2018.1463873.

[10] Y. H. Li, Z. Sheng, P. Zhi, and D. Li, “Multi-objective optimization design of anti-rolling torsion bar based on modified NSGA-III algorithm,” International Journal of Structural Integrity, vol. 12, no. 1, pp. 17–30, Feb. 2021, doi: 10.1108/IJSI-03-2019-0018.
[11] Z. Tang and J. Sun, “Multi objective optimization of railway emergency rescue resource allocation and decision,” International Journal of System Assurance Engineering and Management, vol. 9, no. 3, pp. 696–702, Jun. 2018, doi: 10.1007/s13198-017-0648-y.
[12] E. Altazin, S. Dauzère-Pérès, F. Ramond, and S. Tréfond, “A multi-objective optimization-simulation approach for real time rescheduling in dense railway systems,” Eur J Oper Res, vol. 286, no. 2, pp. 662–672, Oct. 2020, doi: 10.1016/j.ejor.2020.03.034.
[13] W. Zhai, J. Gao, P. Liu, and K. Wang, “Reducing rail side wear on heavy-haul railway curves based on wheel-rail dynamic interaction,” in Vehicle System Dynamics, Taylor and Francis Ltd., May 2014, pp. 440–454. doi: 10.1080/00423114.2014.906633.
[14] G. F. M. Dos Santos, L. A. S. Lopes, E. J. Kina, and J. Tunna, “The influence of wheel profile on the safety index,” in Proceedings of the Institution of Mechanical Engineers, Part F: Journal of Rail and Rapid Transit, Sep. 2010, pp. 429–434. doi: 10.1243/09544097JRRT360.
[15] H. W. X. G. Q. &. Z. W. Zhang, “Joint Maintenance Strategy Optimization for Railway Bogie Wheelset,” Applied Sciences, vol. 12(14), 2022.
[16] P. H. A. Corrêa, P. G. Ramos, R. Fernandes, P. R. G. Kurka, and A. A. dos Santos, “Effect of primary suspension and friction wedge maintenance parameters on safety and wear of heavy-haul rail vehicles,” Wear, vol. 524–525, Jul. 2023, doi: 10.1016/j.wear.2023.204748.
[17] E. A. Lima, L. B. Baruffaldi, J. L. B. Manetti, T. S. Martins, and A. A. Santos, “Effect of truck shear pads on the dynamic behaviour of heavy haul railway cars,” Vehicle System Dynamics, vol. 60, no. 4, pp. 1188–1208, 2022, doi: 10.1080/00423114.2020.1858120.
[18] P. Pacheco, M. V. Lopes, P. H. A. Correa, and A. A. Dos Santos, “Influence of Primary Suspension Parameters on the Wear Behaviour of Heavy-Haul Railway Wheels Using Multibody Simulation,” in International Conference on Electrical, Computer, Communications and Mechatronics Engineering, ICECCME 2023, Institute of Electrical and Electronics Engineers Inc., 2023. doi: 10.1109/ICECCME57830.2023.10252905.
[19] P. A. Pacheco, P. Corrêa, P. Gonzalez Ramos, R. Fernandes, G. Santos, and A. Santos Jr, Effect of transition functions on the dynamic behavior of heavy-haul wagons. 2023.
[20] Vollebregt, E. A. H., C. Weidemann, and A. Kienberger. "Use of" contact" in multi-body vehicle dynamics and profile wear simulation: Initial results." 22nd IAVSD 2011. Manchester Metropolitan University, 2011.
[21] K. Deb, A. Pratap, S. Agarwal, and T. Meyarivan, “A Fast and Elitist Multiobjective Genetic Algorithm: NSGA-II,” 2002.
[22] I.U. of Railways 518, “Testing and approval of railway vehicles from the point of view of their dynamic behaviour - safety - track fatigue - ride quality,” 2005.

[23] Y. Wu, J. Zeng, Q. Wang, R. Luo, and B. Zhu, “Evaluation Methods of Carbody Hunting Instability of Railway Vehicles,” in Lecture Notes in Mechanical Engineering, Springer Science and Business Media Deutschland GmbH, 2020, pp. 908–914. doi: 10.1007/978-3-030-38077-9_105.